Kinetic Modeling of Dynamic Aspects of the Standard NH3-SCR Reaction Over V2O5-WO3/TiO2 and Fe-Zeolite Commercial Catalysts for the Aftertreatment of Diesel Engines Exhausts

I. Nova, M. Colombo, E. Tronconi

Oil & Gas Science and Technology – Rev. IFP Energies nouvelles, Vol. 66 (2011), No. 4, pp. 681-691

DOI: 10.2516/ogst/2011132

IFP Energies nouvelles International Conference
Rencontres Scientifiques d'IFP Energies nouvelles

E-COSM'09 - IFAC Workshop on Engine and Powertrain Control, Simulation and Modeling
E-COSM'09 - Colloque IFAC sur le contrôle, la simulation et la modélisation des moteurs et groupes motopropulseurs

Kinetic Modeling of Dynamic Aspects of the Standard NH_3-SCR Reaction Over V_2O_5-WO_3/TiO_2 and Fe-Zeolite Commercial Catalysts for the Aftertreatment of Diesel Engines Exhausts

I. Nova, M. Colombo and E. Tronconi

Dipartimento di Energia, Laboratorio di Catalisi e Processi Catalitici, Politecnico di Milano, Piazza Leonardo da Vinci 32, 20133 Milano - Italy
e-mail: isabella.nova@polimi.it - massimo.colombo@mail.polimi.it - enrico.tronconi@polimi.it

Résumé — Modélisation cinétique d'aspects dynamiques de la réaction de RCS-NH_3 standard sur des catalyseurs commerciaux V_2O_5-WO_3/TiO_2 et Fe-zéolite pour le post-traitement de gaz d'échappement de moteurs Diesel — Les données cinétiques dynamiques recueillies sur des catalyseurs V_2O_5-WO_3/TiO_2 et Fe-zéolite commerciaux en analysant le RCS-NH_3 standard du NO pour la réduction des NO_x des gaz d'échappement de véhicules ont montré des effets transitoires à basse température, liés à l'action inhibitrice d'ammoniac en excès.

Afin de décrire de tels effets transitoires, une expression de la vitesse spécifique prenant en compte l'inhibition par NH_3 de la réaction de RCS standard est nécessaire pour des modèles mathématiques de convertisseurs par RCS réels. Nous présentons ici une équation de vitesse de type Mars-Van Krevelen à double site pour décrire les caractéristiques dynamiques associées à l'injection et à l'arrêt de l'ammoniac sur des catalyseurs à la fois à base de V et Fe-zéolite.

Abstract — Kinetic Modeling of Dynamic Aspects of the Standard NH_3-SCR Reaction Over V_2O_5-WO_3/TiO_2 and Fe-Zeolite Commercial Catalysts for the Aftertreatment of Diesel Engines Exhausts — *Dynamic kinetic data collected over commercial V_2O_5-WO_3/TiO_2 and Fe-zeolite catalysts analyzing the standard NH_3-SCR of NO for the abatement of NO_x from vehicle exhausts showed transient effects at low temperatures related to the inhibiting action of excess ammonia.*

In order to describe such transient effects, a specific rate expression accounting for NH_3 inhibition of the standard SCR reaction is needed in mathematical models of real SCR converters. We present herein a dual-site Mars-Ven Krevelen-type rate equation suitable to describe dynamic features associated with ammonia injection and shut-off over both V-based and Fe-zeolite catalysts.

NOTATIONS

$E°_{des}$	Activation energy for NH_3 desorption at zero-coverage (J/mol)
E_{NO}	Activation energy for the standard SCR reaction (J/mol)
k_{ads}	Rate constant for NH_3 adsorption rate (1/s)
$k°_{des}$	Pre-exponential factor for NH_3 desorption rate constant (mole/m^3/s)
$k°_{NO}$	Pre-exponential factor for standard SCR reaction rate constant (1/s)
k_{O_2}	Rate parameter in Equation (4) (-)
K_{NH_3}	Rate parameter in Equation (5) (-)
k_{sp}	Rate constant for NH_3 spillover rate (mole/m^3/s)
p_{O_2}	Partial pressure of O_2 (-)
r_{ads}	Rate of NH_3 adsorption (mol/m^3/s)
r_{des}	Rate of NH_3 desorption (mol/m^3/s)
r_{NO}	Rate of standard SCR reaction (mol/m^3/s)
r_{Spill}	Rate of ammonia spillover reaction (mol/m^3/s)
T	Temperature (K)
α	Parameter for surface coverage dependence, Equation (2) (-)
θ_{NH_3}	NH_3 surface coverage on S_2 sites (-)
σ	NH_3 surface coverage on S_1 sites (-)

INTRODUCTION

Diesel engines, being inherently more thermodynamically efficient than petrol engines, offer the prospect of reducing fuel consumption and emissions of carbon dioxide as well. Indeed, they are fated to significantly increase their world-wide penetration on light duty vehicles [1], while they already monopolize the market for heavy duty ones.

On the other hand, Diesel engines produce higher emissions of nitrogen oxides (NO_x) and particulates. Improvements in combustion and/or alternative fuels can lead to lower NO_x emissions, but it is widely accepted that, in order to meet the future legislative standards (Euro 6 for light duty and Euro VI for heavy duty vehicles, as well as US 2010 Bin5), the adoption of aftertreatment systems will be required to reduce both NO_x and particulate emissions [1].

Concerning NO_x reduction, there are different major aftertreatment technologies presently under consideration: the NO_x adsorbers, which are used with direct injection gasoline and Diesel engines, the HC-SCR catalysts for light-duty Diesel engines, and the Selective Catalytic Reduction (SCR) process [1].

SCR was the European motor industry's main technology choice to meet Euro 4 and Euro 5 emissions requirements for heavy-duty Diesel engines, and recently it has been announced by some manufacturers for passenger cars in the US and in Europe, as well [1]. An SCR system is designed to catalytically reduce NO_x emissions in the oxygen rich environment of Diesel exhausts. To reduce NO_x emissions, the SCR system needs a chemical reagent, or reductant, to help convert the NO_x to nitrogen: in mobile source applications the preferred reductant is typically an aqueous solution of non-toxic urea that is used as ammonia source. In current technologies, the so-called Adblue® solution is injected into the exhaust system, where it is decomposed to NH_3.

Most of the NO_x emitted by the engine consist of nitric oxide (NO). However, upstream of the SCR converter, a Diesel Oxidation Catalyst is typically present in the system configuration, that allows the partial conversion of NO to NO_2; this permits the occurrence of the fast SCR reaction:

$$2NH_3 + NO + NO_2 \rightarrow 2\ N_2 + 3\ H_2O \qquad (1)$$

very active already at low temperature, in addition to the well known standard SCR reaction:

$$2\ NH_3 + 2\ NO + {}^1/_2\ O_2 \rightarrow 2\ N_2 + 3\ H_2O \qquad (2)$$

The SCR technology was first brought to the market in 2005 for heavy duty vehicle applications by Daimler under the trade mark BLUETEC®, based on the use of extruded honeycomb monolith catalysts consisting of V_2O_5-WO_3/TiO_2. The application of such a new technology was optimized by using an unsteady kinetic model of the SCR process specifically developed for mobile applications: indeed, simulation tools able to describe the performance of catalytic converters as a function of the several operating parameters have been proven very useful in the development and design of aftertreatment systems. Nevertheless, the capability of such models in predicting accurately NO_x and ammonia emissions mainly relies on the close adherence of kinetic schemes to the real catalytic process.

More recently, new catalysts are being considered for the NH_3-SCR reactions for mobile applications, such as metal-promoted zeolites. Among these, the Fe-promoted zeolite system is known for its very high activity in the presence of NO_2, high selectivity to dinitrogen also at high temperatures, and high thermal durability.

In this paper we present the development of unsteady kinetic models of the NH_3-SCR process for both vanadium-based and Fe-zeolite catalysts, specifically addressing the transient effects observed at low temperatures in the case of the simpler NO/NH_3-O_2 reacting system. Indeed, although SCR systems for mobile applications are typically designed to promote the fast SCR reactivity, the NO_2 concentration at SCR inlet can also be very low (*e.g.* low activity of the upstream DOC at low temperature); under these conditions the dynamics related to the standard SCR reaction can become dramatically important.

The presented models implement kinetic schemes derived from an extensive investigation of reactivity, chemistry and catalytic mechanism of all the main SCR reactions over commercial V_2O_5-WO_3/TiO_2 and Fe-zeolite catalysts performed in our laboratories during the last few years [2-14].The related rate expressions were fitted to transient data collected over powdered catalysts in the chemical regime, and in their global form allow the kinetic analysis of the full NH_3–NO/NO_2 SCR reacting system.

The intrinsic kinetic models, as well as the relevant geometrical and morphological characteristics of the monolith commercial catalysts, were then incorporated into a fully transient heterogeneous 1D+1D mathematical model of SCR monolith reactors, which was validated against transient SCR runs performed at different scales, eventually including test bench data collected on full scale SCR monolith converters, using real Diesel engine exhaust gases [2-4, 10, 11, 13].

1 METHODS

1.1 Experimental Procedures

Unsteady kinetic SCR experiments of various nature were performed in the 50-550°C *T*-range over commercial V_2O_5-WO_3/TiO_2 and Fe-zeolite catalysts, originally supplied by Daimler as extruded and washcoated honeycomb monoliths, respectively. The monolith catalysts were crushed and ground to powder (140-200 mesh), a sample of powder (160 mg for vanadium-based and 80 mg for Fe-zeolite catalysts) was diluted with 80 mg of quartz and loaded in a flow-microreactor consisting of a quartz tube (6 mm *i.d.*) directly connected both to a UV analyzer (ABB Limas 11-HW) and to a quadrupole mass spectrometer (Balzers QMS 200), which operated in parallel [14].

The dynamics of the SCR reactions were investigated using Transient Response Methods (TRM), that consist in performing stepwise changes of concentration of one species in the feed mixture by means of fast response pulse valves at constant temperature. TRM runs were typically carried out in the presence of oxygen (2% v/v) and water vapor (1 or 3% v/v) in the temperature range 150-500°C, while the feed concentrations of NH_3 and NO_x were varied between 0 and 500 or 1000 ppm. A Gas Hourly Space Velocity (GHSV) between 194 000 and 890 000 $cm^3/(h\ g_{cat})$ was used in all the experiments. Further experimental details can be found elsewhere [10, 11, 15].

Catalyst conditioning consisted in a temperature ramp of 5 K/min from room temperature up to 600°C in 10% O_2 v/v + 10% v/v H_2O, followed by hold at 600°C for 5 h.

Intraparticle gradients and gas-solid mass and heat transfer limitations in the powdered catalyst bed were ruled out by diagnostic criteria [16]. An analysis of the mass transport limitations in microreactor experiments over the V_2O_5-WO_3/TiO_2 catalyst can be found in [11]. For the Fe-zeolite catalyst the same procedure was adopted, based on estimates of the species effective diffusivities of the order of 10^{-7} m^2/s at 200°C.

The SCR reactions were also investigated over core drilled monolith samples (with square section 11.5 × 11.5 mm, and 50 mm length) under isothermal steady-state conditions within the 150-550°C *T*-range, using a different rig. The catalyst conditioning procedure was the same as for the powder samples. Typical feed concentrations of NO_x and NH_3 were 500-1 000 ppm, O_2 2-10% v/v and water 1-10% v/v, with balance N_2. Analysis of the outlet gases was performed using a UV-analyzer (ABB LIMAS 11HV) directly connected to the reactor outlet via a heated line.

1.2 Kinetic Analysis

The transient data collected over the powdered SCR catalysts were analyzed according to a dynamic one-dimensional isothermal isobaric heterogeneous plug-flow model of the test microreactor in order to obtain estimates of the relevant SCR rate parameters [2-4].

The complete models [4, 11] included several kinetic steps, in order to fully describe the NH_3–NO-NO_2/O_2 reacting system in the whole *T*-range; Table 1 shows the steps necessary to analyse the simpler NH_3–NO/O_2 reacting system, while in Table 2 the corresponding rate expressions are reported. The orders of magnitude of the estimated rate parameters for both the V_2O_5-WO_3/TiO_2 catalyst and the Fe-zeolite one can be found respectively in [11] and [4].

The rate expression of step R.4 has been derived assuming that two different types of sites are available on the catalyst surface: one Redox site for O_2 and NO adsorption/reaction (S1), likely associated with V or Fe, and one acidic site for NH_3 adsorption (S2) associated with the W or Ti and zeolite material.

TABLE 1

List of reactions included in the kinetic model (NH_3–NO/O_2 reacting system)

R.1	$S_2 + NH_3 \rightarrow S_2[NH_3]$	NH_3 adsorption	r_{ads}
R.2	$S_2[NH_3] \rightarrow S_2 + NH_3$	NH_3 desorption	r_{des}
R.3	$S_2[NH_3] + {}^3/_4\ O_2 \rightarrow {}^1/_2\ N_2 + {}^3/_2\ H_2O$	NH_3 oxidation	r_{ox}
R.4	$S_1[NO] + S_2[NH_3] + {}^1/_4\ O_2 \rightarrow N_2 + {}^3/_2\ H_2O + S_1 + S_2$	Standard SCR	r_{NO}
R.5	$S_2[NH_3] + S_1 \leftrightarrow S_2 + S_1[NH_3]$	NH_3 spillover	r_{spill}

Briefly, a weak NO adsorption occurs onto S_1 sites, while on adjacent S_2 sites NH_3 is strongly adsorbed; then, the $DeNO_x$ step (NO + NH_3) involves reduction of the S_1 sites, followed by reoxidation of reduced S_1 sites by gaseous oxygen [10].

TABLE 2

List of rate expressions (NH_3–NO/O_2 reacting system)

R.1	$r_{ads} = k_{ads} C_{NH_3} (1 - \theta_{NH_3})$	Eq. (1)
R.2	$r_{des} = k^{\circ}_{des} \exp\left[-\frac{E^{\circ}_{des}}{RT}(1 - \alpha\theta_{NH_3})\right]\theta_{NH_3}$	Eq. (2)
R.3	$r_{ox} = k_{ox}\theta_{NH_3}(p_{O_2}/0.02)^{\beta}$	Eq. (3)
R.4	$r_{NO} = \frac{k^{\circ}_{NO} \cdot e^{-E^{\circ}_{NO}/RT} C_{NO}\theta_{NH_3}}{\left(1 + k_{O_2}\frac{C_{NO}\theta_{NH_3}}{C^{1/4}_{O_2}}\right)}(1 - \sigma_{NH_3})$	Eq. (4)
R.5	$r_{spill} = k_{sp}\left[\theta_{NH_3}(1 - \sigma_{NH_3}) - \frac{\sigma_{NH_3}(1 - \theta_{NH_3})}{K_{NH_3}}\right]$	Eq. (5)

In addition, a reversible "NH_3 spillover" step R.5 from S_2- to S_1-sites, which results in blocking the active redox sites, was included in the scheme in order to account for ammonia inhibition effects (vide infra).

Starting from this Redox scheme, and using a Mars-Van Krevelen formalism, the reaction rate expression of the standard SCR reaction Equation (4), also referred to as Modified Redox rate law (MR), has been derived [10]. Also a kinetic approach was assumed for NH_3 spillover, which eventually leads to Equation (5), rate expression for step (R.5).

Indeed, the evaluation of the SCR rate r_{NO} according to Equation (4) requires time integration of Equation (5).

It is important to notice that the complex rate expression Equation (4) can be simplified. *E.g.* at low ammonia coverages, as typical of temperatures above 250-300°C, it reduces to the well known Eley Rideal rate law (ER):

$$r_{NO} = k_{NO} \cdot C_{NO} \cdot \theta_{NH_3} \qquad \text{Eq. (6)}$$

in which one molecule of adsorbed ammonia species reacts with one molecule of gaseous NO; such an expression is commonly used in the kinetic literature for SCR stationary applications [17], which indeed typically work under steady conditions in the 250-400°C *T*-range.

1.3 Test Reactor Model

The test reactor model comprises the transient 1D mass balance equations of adsorbed and of gaseous species. The set of Partial Differential Equations, with obvious initial and boundary conditions, was solved numerically according to the method of lines, based on axial discretization with backward finite differences and on time integration by Gear's algorithm.

The kinetic parameters for ammonia adsorption-desorption and for ammonia oxidation were estimated on the basis of kinetic runs performed by feeding only NH_3 in the presence of O_2 and water. As an example, Figure 1 shows a typical adsorption/temperature programmed desorption test over the Fe-zeolite catalyst used for the estimation of NH_3 adsorption/ desorption rate parameters, in comparison with the corresponding kinetic fit.

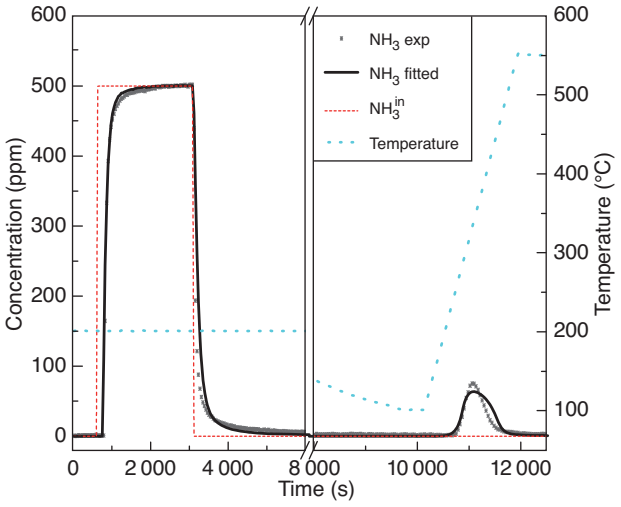

Figure 1

NH_3 adsorption-desorption + TPD run over the Fe-zeolite catalyst. NH_3 = 500 ppm, O_2 = 2% v/v (0% during TPD), H_2O = 3% v/v, Q = 71 Ncc/min. He carrier gas. Dots: experimental data; dashed line: inlet concentration; thick line: kinetic fit using the Double Horn model. Adapted from Reference [15].

Concerning the estimation of the rate parameters in the remaining rate expressions for the SCR reactions, the temporal evolutions of the outlet NH_3, NO, N_2 concentrations were used as fitted responses in a global multiresponse nonlinear regression of different TRM experiments performed varying temperature, the NO_2/NO_x feed ratio, ammonia, NO_x and O_2 concentrations, using a robust multimethod regression routine [18].

1.4 Transport Model

The model of the honeycomb monolith SCR converter is an heterogeneous dynamic 1D+1D model of a single monolith channel: it includes the unsteady differential mass balance equations of gaseous species and of adsorbed species. Rate equations are exactly those determined from kinetic runs at the microreactor scale. Enthalpy balances for the gas and for the solid phase are included to account also for thermal effects. In addition, intra-phase diffusional limitations are accounted for by equations for diffusion-reaction of the gaseous reactants in the porous catalytic monolith wall or washcoat, with effective diffusivities evaluated from the

catalyst morphological data according to a modified Wakao-Smith random pore model [19]. The resulting set of model PDEs was solved numerically according to the method of lines, applying orthogonal collocation techniques to the discretization of the unknown variables along both the z (axial) and x (intraporous) coordinates, and integrating the resulting ODEs in time by Gear's algorithm for stiff systems.

2 RESULTS AND DISCUSSION

2.1 Transient Experiments Over the V-based Catalyst

The NH_3, NO and N_2 concentration profiles *versus* time collected in transient reaction experiments at different temperatures feeding NO and NH_3 in the presence of different oxygen feed contents are shown as symbols in Figures 2 (O_2 = 2% v/v) and 3 (O_2 = 6% v/v). In all cases, 1 000 ppm ammonia were fed to the reactor in a stepwise manner while flowing 1 000 ppm of NO + O_2 + 1% v/v H_2O.

In all the experiments, upon NH_3 step feed the NH_3 outlet concentration trace exhibited a dead time and then slowly grew with time on stream, eventually approaching a steady-state value. In parallel, a fast decrease in the NO outlet concentration together with a mirror-like increment of the N_2 concentration, associated with the startup of the SCR reaction were observed. The levels of NH_3, NO and N_2 at steady-state were in all cases consistent with the stoichiometry of the standard SCR reaction (2) [2, 3, 5, 10, 12, 13, 20, 21]. Results obtained in the presence of different oxygen contents were qualitatively very similar. The main effect of the higher oxygen concentration was a slight enhancement of the SCR conversion, as measured by the steady state levels of ammonia, NO and nitrogen: for example, at 250°C a conversion less than 80% was measured at steady state when 2% oxygen was fed to the reactor, while in the presence of 6% of oxygen

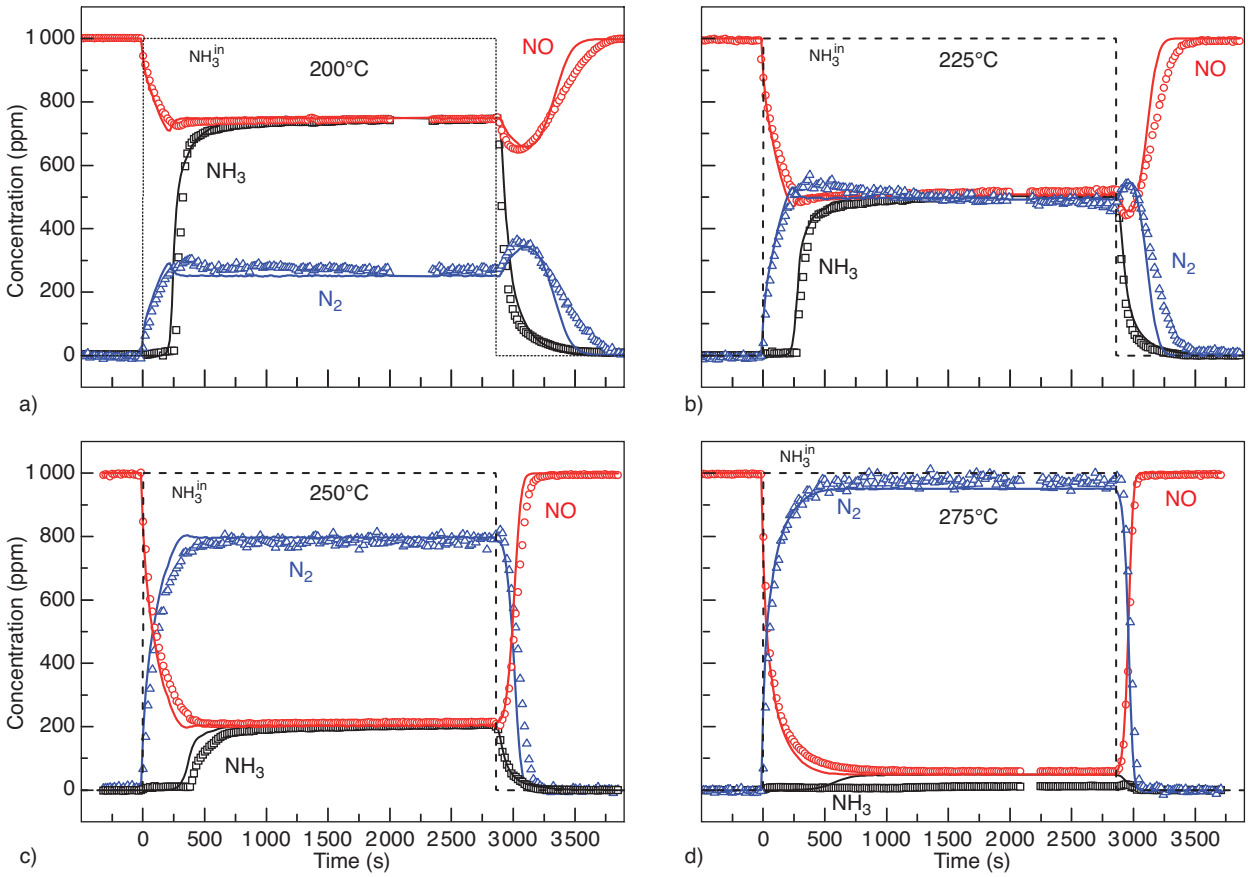

Figure 2

Transient SCR microreactor experiments over the V-based catalyst with step feed of NH_3 (0-1 000 ppm) in NO (1 000 ppm) + O_2 (2% v/v) and H_2O (1% v/v) + He at different temperatures. Symbols: measured concentrations of NH_3, NO, N_2 at reactor outlet. Lines: kinetic fit using Equation (4) (Modified Redox rate law). Adapted from Reference [10].

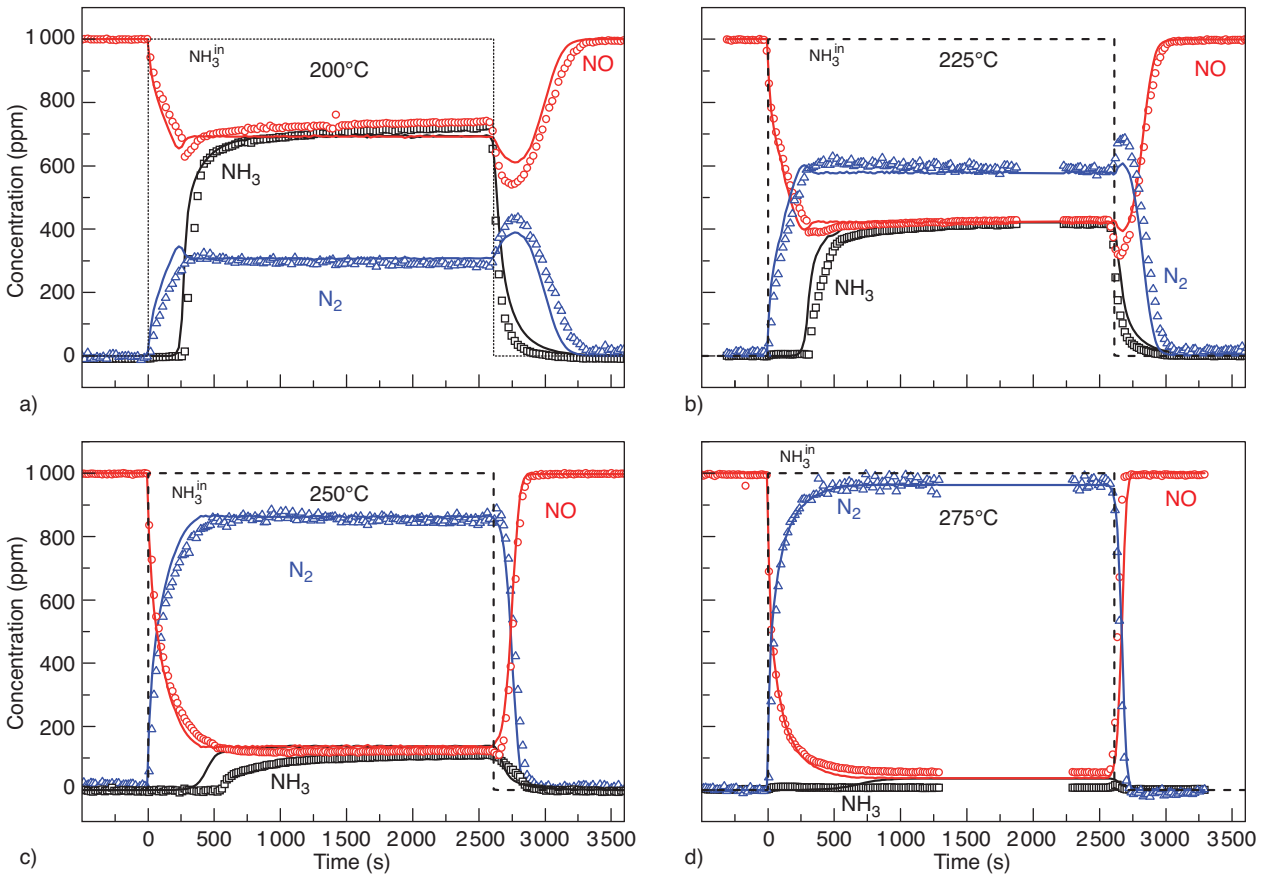

Figure 3

Transient SCR microreactor experiments over the V-based catalyst with step feed of NH_3 (0-1 000 ppm) in NO (1 000 ppm) + O_2 (6% v/v) and H_2O (1% v/v) + He at different temperatures. Symbols: measured concentrations of NH_3, NO, N_2 at reactor outlet. Lines: kinetic fit using Equation (4) (Modified Redox rate law). Adapted from Reference [10].

such a value was increased to almost 85%. On the other hand, a significant effect of temperature was evident: above 225°C the temperature affected the SCR reaction only by increasing the NO and ammonia conversions. As opposite, in the low *T*-range a different dynamic behavior of NO and N_2 was observed during both the NH_3 start-up phase and the NH_3 shut-off.

Figure 4a focuses on the experiment run at 200°C with 2% oxygen: when ammonia was added to the feed flow (t = 0 s) the NO concentration (paralleled by the N_2 formation) decreased, went through a minimum, and then reached an higher steady state value; at ammonia shutdown the NO concentration (and symmetrically the N_2 production) decreased significantly passing through a minimum, then began to increase and approached its inlet value. Such an effect was observed in the runs with both 2 and 6% oxygen, indicating that oxygen content did not alter the dynamic features of the transient experiments at low temperature.

Further experiments were performed with high frequency NH_3 feed pulses in a stream of 1 000 ppm of NO, 2% v/v O_2 and 1% v/v H_2O *(Fig. 4b)*. The results (symbols) showed again the characteristic transient behaviour associated with ammonia addition and removal from the feed flow: the greatest NO conversion was always reached during each pulse after the NH_3 shut down.

Thus it appears the $DeNO_x$ activity of the system was temporarily hindered by excess ammonia, as already pointed out by other authors on different systems [22-26], suggesting the existence of an optimal ammonia surface concentration, which is lower than the coverage established at steady state. This behavior was attributed to an ammonia inhibition effect, *e.g.* due to electronic interaction or possibly via direct blocking of the redox sites.

Figure 5 (thin solid and dashed lines) shows the evolution of NO conversion as a function of the NH_3 surface concentration during the NH_3 feed and shut-off transients of the

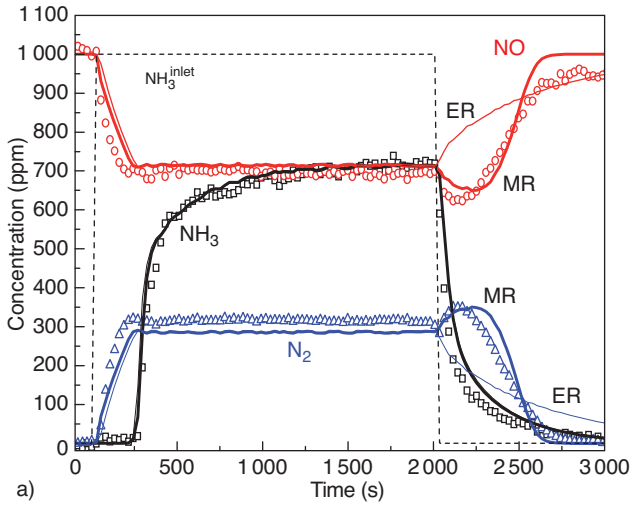

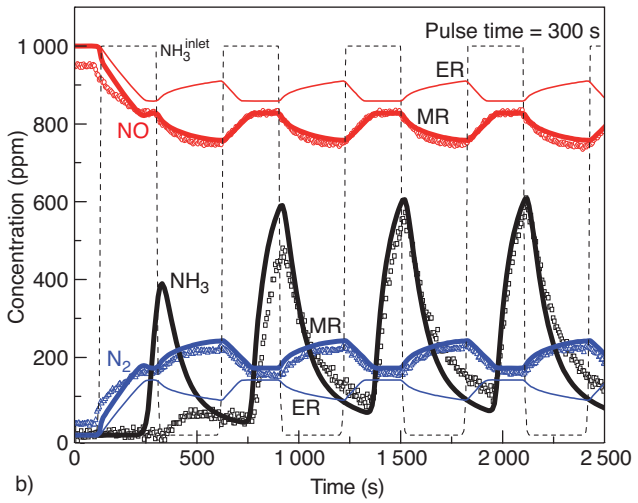

Figure 4

Isothermal transient experiments over the V-based catalyst with steps feed of NH_3. T = 200°C, NH_3 = 0-1 000 ppm, NO = 1 000 ppm, O_2 = 2% v/v, H_2O = 3% v/v, He carrier gas. a) Ammonia pulse of about 2 000 s; b) ammonia pulses of 150 s. Symbols: measured concentrations of NH_3, NO, N_2 at reactor outlet. Lines ER: kinetic fit using Equation (6) (Eley-Rideal rate law). Lines MR: kinetic fit using Equation (4) (Modified Redox rate law). Adapted from References [10, 13].

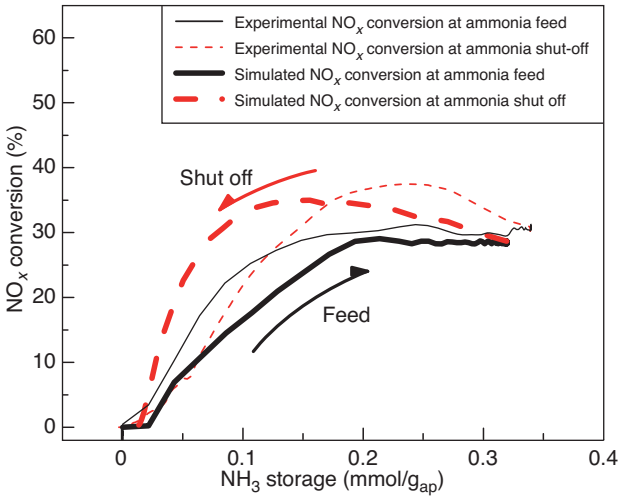

Figure 5

NO_x conversion coverage dependence during transient experiment of Figure 2a: microreactor experiment with step feed of NH_3 (0-1 000 ppm) in NO (1 000 ppm) + O_2 (2% v/v) and H_2O (1% v/v) + He at 200°C. Thin lines: measured NO_x conversion; thick lines: kinetic fit using Equation (4) (Modified Redox rate law); solid lines: NO_x conversion during ammonia feed; dashed lines: NO_x conversion during ammonia shut-off.

TRM run performed at 200°C presented in Figure 3a. The NH_3 surface concentration was calculated from the integral difference between inlet and outlet concentrations, taking into account that a part of the NH_3 fed to the reactor was converted to nitrogen according to the stoichiometry of the Standard SCR reaction.

Looking at the solid line obtained during the NH_3 feed transient, it can be seen that the NO conversion increased up to about 30% for an ammonia surface concentration of 0.15-0.2 mmol/g and then remained more or less stable. Interestingly, the NO evolution during the following NH_3 shut-off transient (thin red dashed line) exhibited a different behaviour, with maximum NO conversion close to 40% for an ammonia surface concentration of about 0.23 mmol/g pointing out that different NO_x conversions could be associated with the same NH_3 surface concentration during transients, thus resulting in a hysteresis behaviour.

Solid lines in Figures 2-5 (MR thick lines) represent the data fit obtained using the MR kinetics, Equation (4). A satisfactory agreement was achieved between experimental and calculated data in the experiments run in the presence of both 2 and 6% oxygen. It is worth of note that the MR rate expression *(Eq. 4)*, relying on the assumption that the SCR reaction is governed by a redox mechanism, could nicely predict the kinetic dependence on oxygen. Furthermore, as more evident from Figures 4 and 5, the MR rate law captured nicely the complex maxima-minima features of the experimental NO and N_2 traces at low T at both NH_3 startup and shutdown. Focusing on Figure 5, it appears that the MR rate expression (thick lines) is able to qualitatively and quantitatively reproduce the observed NO conversion coverage dependence during both NH_3 feed and shut-off transients. In accordance with the experimental data, the model predicts a hysteresis, with a higher NO conversion during the NH_3 shut off transient (red thick dashed line).

For comparison purposes, Figure 4 also shows the results of a fit performed adopting an Eley Rideal rate expression (ER thin lines, *Eq. 6*) to describe the NO consumption. It appears that in this case a satisfactory agreement was achieved between experimental data and model fit at steady state, but not in the case of the transient associated with the ammonia inhibition effect, which indeed is not taken into account in Equation (6).

2.2 Transient Experiments Over the Fe-Zeolite Catalyst

In analogy with what done over the V-based catalyst, different sets of isothermal transient experiments were performed at different temperatures over the Fe-zeolite catalyst by feeding in a stepwise manner 500 ppm of NH_3 while continuously flowing 500 ppm of NO in the presence of oxygen (2%), water (3%) and balance helium.

The NH_3, NO, N_2 and N_2O (symbols) concentration profiles *versus* time collected in transient reaction experiments with ammonia pulses of different lengths at 200 and 250°C are shown in Figures 6 and 7, respectively.

In the run at 200°C (NH_3 step feed at 2 700 s in a flow of NO, oxygen and water, Figure 6a), as soon as ammonia was fed to the reactor the outlet concentration trace exhibited about 25 s of dead time and then slowly grew with time on stream, eventually approaching a steady-state value of about 480 ppm. At the same time, the NO signal rapidly went through a minimum before eventually approaching the steady state value of about 480 ppm; the nitrogen signal mirrored that of NO. During both the dynamic phase and the steady state condition the concentrations of NO, NH_3 and N_2 were consistent with the stoichiometry of the Standard SCR reaction (2), indicating a NO_x conversion of ~4%. A maximum in the $DeNO_x$ activity, with a simultaneous nitrogen peak, were also noticed at NH_3 shut-off, while the NH_3 concentration rapidly dropped to zero. As already pointed out in the case of the V-based catalyst, the temporary enhancements in the $DeNO_x$ activity observed over the Fe-zeolite catalyst both at NH_3 opening and shut off are likely associated with an inhibiting effect played by excess NH_3 present on the catalyst surface or in the gas phase [4, 6-8, 26, 27].

In Figures 6b, c, the results collected at 200°C by adding and removing NH_3 from the feed stream every 300 and 150 s, respectively, are reported. Data shows that the transient features observed at NH_3 opening and shut off were still present and comparable with those already discussed in the case of a longer NH_3 feed: a maximum in the $DeNO_x$ activity was always reached when NH_3 entered the reactor and also when it was removed from the feed flow. Also, the steady state conversion achieved at the end of each transients remained unaltered. However, the increase of $DeNO_x$ activity during the dynamics leads to an increase of the time-averaged NO conversion.

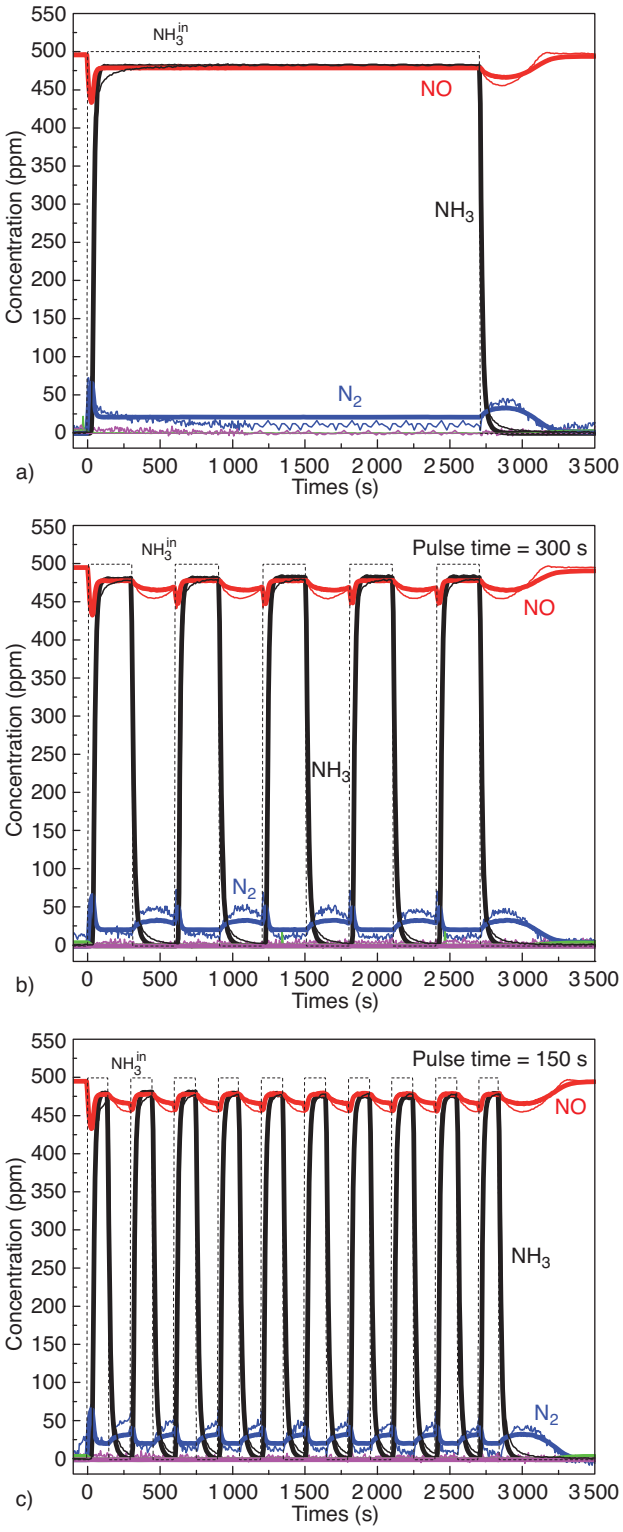

Figure 6

Isothermal transient experiments with steps feed of NH_3. T = 200°C, NH_3 = 500 ppm, NO = 500 ppm, O_2 = 2% v/v, H_2O = 3% v/v, Q = 327 Ncc/min, He carrier gas. Thin lines: experimental data; thick lines: kinetic fit using Equation (4) (Modified Redox rate law). a) Ammonia pulse of about t = 2 750 s; b) ammonia pulses of 300 s; c) ammonia pulses of 150 s. Adapted from Reference [15].

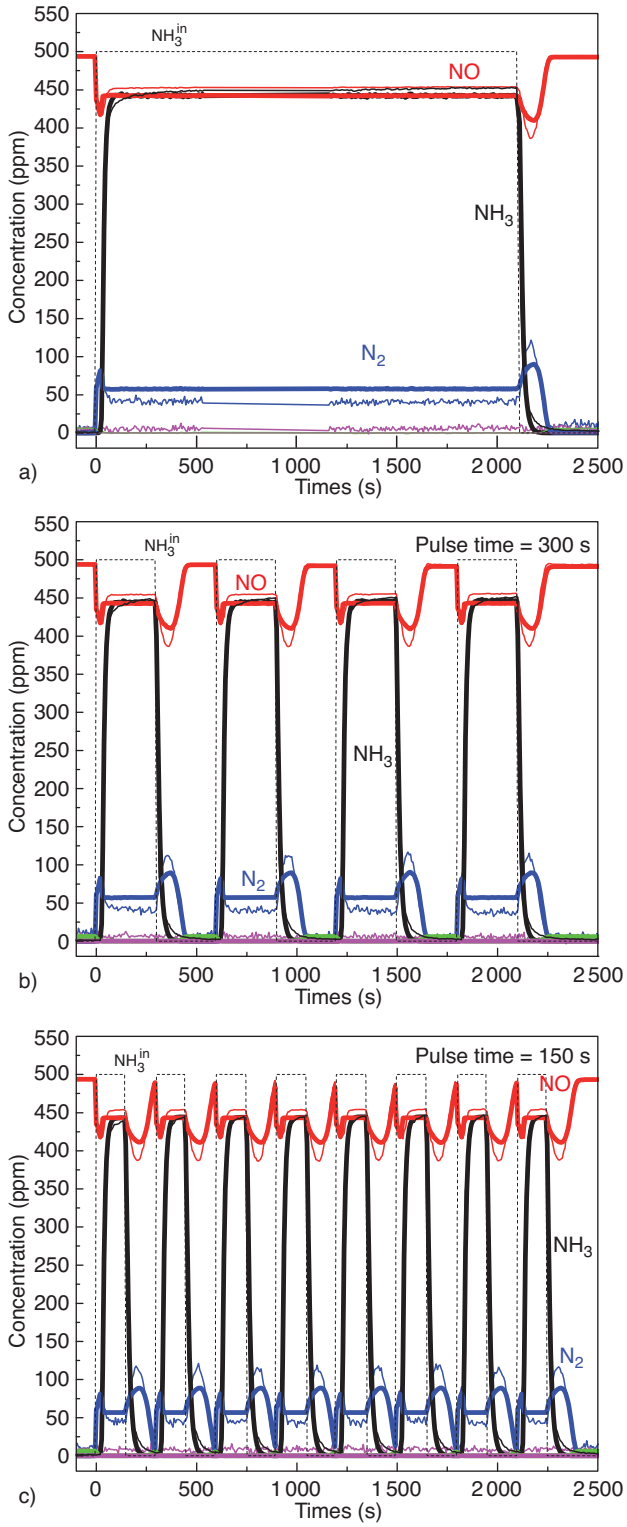

Figure 7

Isothermal transient experiments with steps feed of NH_3. T = 250°C, NH_3 = 500 ppm, NO = 500 ppm, O_2 = 2% v/v, H_2O = 3% v/v, Q = 327 Ncc/min, He carrier gas. Thin lines: experimental data; thick lines: kinetic fit using Equation (4) (Modified Redox rate law). a) Ammonia pulse of about t = 2 100 s; b) ammonia pulses of 300 s; c) ammonia pulses of 150 s. Adapted from Reference [15].

Figures 7a-c (symbols) show similar experiments performed at 250°C. The temperature did not affect qualitatively the transient effects in the outlet concentration profiles of NO and nitrogen. However, such dynamics became less pronounced as the temperature increased. In parallel, the temperature positively affected the NO_x conversion, which increased from 4% at 200°C to 10% at 250°C.

The similarities between the dynamics observed in the case of vanadium based catalysts and over the present Fe-zeolite system suggest that the NH_3 inhibition invoked for V_2O_5-WO_3/TiO_2 can apply to Fe-promoted zeolites as well. Indeed, it is well known in the literature that the presence of suitable metals (Fe, Cu) in the zeolite framework greatly enhances the SCR activity [30], while it is well established that NH_3 easily adsorbs onto the acidic sites of the zeolite [31, 32]. However, it has been reported in the literature that NH_3 is able to adsorb on the Fe sites, too [33]. We can thus speculate that, in analogy with vanadium based catalysts, the Standard SCR rate-limiting step occurs on Fe-sites involving a redox catalyst function. The adsorption/interaction of NH_3 with these sites may result in blocking of the redox function, thus causing a decrease of the $DeNO_x$ activity. Accordingly, the same Modified redox kinetic scheme originally developed for the vanadium based catalyst has been applied to the Fe-zeolite system.

The solid lines in Figure 6 and 7 show the corresponding model fits. The model was indeed able to reproduce qualitatively and quantitatively the different transient effects in the NO and N_2 concentration profiles observed both at NH_3 opening and shutoff over the Fe-zeolite catalyst as well. The effects both of the NH_3 pulse length and of temperature on the system dynamics were nicely captured by the Modified Redox kinetic model.

2.3 Model Validation

The derived kinetic model was eventually validated by performing additional runs both over a powdered catalyst at the microreactor scale and over monolith catalysts, and comparing them with the corresponding simulations. The same isothermal Plug Flow reactor model employed for the kinetic fit was used for the simulations of the microreactor experiments, while a fully transient heterogeneous 1D+1D model of SCR monolith reactors [2-4, 13, 15] was employed for simulation of the experiments performed over structured systems, accounting also for mass transfer effects in the monolith catalyst.

Figure 8 shows as an example part of a validation run over a small core sample of the monolith Fe-zeolite catalyst: pulses of 750 ppm NH_3 (5 min on/5 min off) were added to a continuous feed stream containing 500 ppm NO, 8% v/v H_2O, 8% v/v O_2 and balance N_2 at 250°C. A good agreement is apparent between the experimental traces

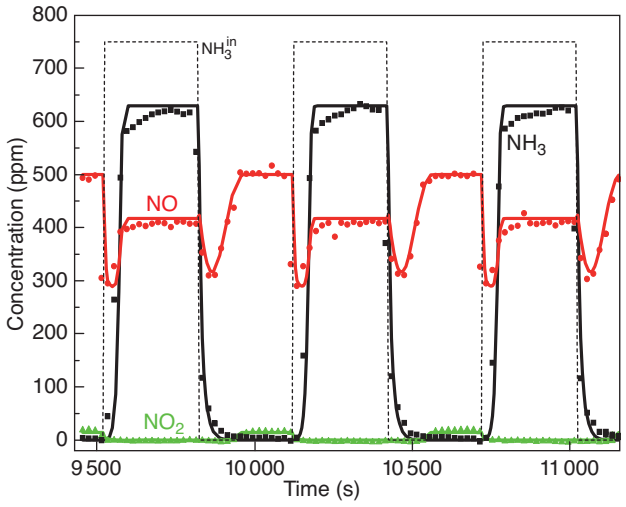

Figure 8

Isothermal transient experiments with steps feed of NH_3 over Fe-zeolite monolith. T = 250°C, NH_3 = 750 ppm, NO = 500 ppm, O_2 = 8% v/v, H_2O = 8% v/v, GHSV = 75 300 h^{-1}, N_2 carrier gas; ammonia pulses of 300 s. Symbols = experimental data; thick lines: model simulations.

(symbols) and the model predictions (solid lines) of NO and ammonia outlet concentrations. Overall, the very demanding transient features associated with the instantaneous changes in the NH_3 feed concentration were well reproduced by the model.

Transient test bench validation runs were carried out over the same commercial SCR catalysts used for the kinetic study, but in the shape of full scale honeycomb monoliths, feeding real engine exhausts [2-4, 13, 15]. In particular, it has to be noticed that both over the small core samples and over the full scale monolith catalysts the transient effects related to ammonia injection and shut off, associated with NH_3 inhibition effects, were quite evident. The Modified Redox rate expression developed to take into account such ammonia inhibition effect was indeed able to simulate on a pure predictive basis also the dynamic features observed at the real scale.

In all cases and over both the vanadium based and the Fe-zeolite catalyst, a general good correlation between simulation and experiment was obtained, being the mean deviation in NO_x and ammonia concentrations always below 5%, thus validating the model in the explored temperature and concentration ranges and proving the effectiveness of the scale-up procedure.

CONCLUSIONS

Dynamic kinetic data collected over commercial V_2O_5-WO_3/TiO_2 and Fe-zeolite catalysts showed transient effects related to inhibition by excess ammonia. Accordingly, a specific rate expression accounting for NH_3 inhibition of the Standard SCR reaction is needed in mathematical models of real SCR converters.

For this purpose, an original, dual-site Mars-Van Krevelen unsteady kinetic model of the standard SCR reaction over both vanadium based and Fe-zeolite catalysts for the abatement of NO_x emissions from the exhausts of Diesel engines was derived, based on large experimental data sets collected under chemical regime over powdered catalysts and validated against runs performed over small and full-scale monolith catalyst samples. The standard SCR kinetic model was able to reproduce successfully not only the steady state behaviours, but also the detailed and complex transient features observed during dynamic runs at low temperatures.

The model herein reported for the standard SCR reaction only is part of a more complex kinetic model, chemically consistent with a redox catalytic mechanism proposed on the basis of an extensive investigation of reactivity, chemistry and catalytic mechanism of the full NH_3–NO/NO_2 SCR reacting system over both V_2O_5-WO_3/TiO_2 and Fe-zeolite catalysts performed in our laboratories: it fully accounts for stoichiometry, selectivity and kinetics of the global NH_3-NO/NO_2 SCR process. The complete model was also successfully validated at the real converter scale, taking into account mass and heat transfer effects, and is currently applied to the development of industrial SCR technologies for vehicles.

ACKNOWLEDGMENTS

Daimler AG is gratefully acknowledged for financial support.

REFERENCES

1 Johnson T. (2010) Review of Diesel Emissions and Control, *SAE Technical Paper* 2010-01-0301.

2 Chatterjee D., Burkhardt T., Bandl-Konrad B., Braun T., Tronconi E., Nova I., Ciardelli C. (2005) Numerical simulation of ammonia SCR catalytic converters: model development and application, *SAE Technical Paper* 2005-01-0965.

3 Chatterjee D., Burkhardt T., Weibel M., Tronconi E., Nova I., Ciardelli C. (2006) Numerical simulation of $NO/NO_2/NH_3$ reactions on SCR catalytic converters: Model development and applications, *SAE Technical Paper* 2006-01-0468.

4 Chatterjee D., Burkhardt T., Weibel M., Nova I., Grossale A., Tronconi E. (2007) Numerical simulation of zeolite and V-based SCR catalytic converters, *SAE Technical Paper* 2007-01-1136.

5 Ciardelli C., Nova I., Tronconi E., Chatterjee D., Bandl-Konrad B., Weibel M., Krutzsch B. (2007) Reactivity of NO/NO_2-NH_3 SCR system for diesel exhaust aftertreatment: Identification of the reaction network as a function of temperature and NO_2 feed content, *Appl. Catal. B: Env.* **70**, 1-4, 80-90.

6 Colombo M., Nova I., Tronconi E. (2010) A comparative study of the NH_3-SCR reactions over a Cu-zeolite and a Fe-zeolite catalyst, *Catal. Today* **151**, 3-4, 223-230.

7 Grossale A., Nova I., Tronconi E. (2008) Study of a Fe-zeolite-based system as NH_3-SCR catalyst for diesel exhaust aftertreatment, *Catal. Today* **136**, 1-2, 18-27.

8 Grossale A., Nova I., Tronconi E., Chatterjee D., Weibel M. (2008) The chemistry of the NO/NO_2-NH_3 "fast" SCR reaction over Fe-ZSM5 investigated by transient reaction analysis, *J. Catal.* **256**, 2, 312-322.

9 Nova I., Ciardelli C., Tronconi E., Chatterjee D., Bandl-Konrad B. (2006) NH_3-NO/NO_2 chemistry over V-based catalysts and its role in the mechanism of the Fast SCR reaction, *Catal. Today* **114**, 1, 3-12.

10 Nova I., Ciardelli C., Tronconi E., Chatterjee D., Bandl-Konrad B. (2006) NH_3-SCR of NO over a V-based catalyst: Low-T redox kinetics with NH_3 inhibition, *AIChE J.* **52**, 9, 3222-3233.

11 Nova I., Ciardelli C., Tronconi E., Chatterjee D., Weibel M. (2009) Unifying Redox Kinetics for Standard and Fast NH_3-SCR over a V_2O_5-WO_3/TiO_2 Catalyst, *AIChE J.* **55**, 6, 1514-1529.

12 Tronconi E., Nova I., Ciardelli C., Chatterjee D., Weibel M. (2007) Redox features in the catalytic mechanism of the "standard" and "fast" NH_3-SCR of NO_x over a V-based catalyst investigated by dynamic methods, *J. Catal.* **245**, 1, 1-10.

13 Tronconi E., Nova I., Ciardelli C., Chatterjee D., Bandl-Konrad B., Burkhardt T. (2005) Modelling of an SCR catalytic converter for diesel exhaust after treatment: Dynamic effects at low temperature, *Catal. Today* **105**, 3-4, 529-536.

14 Ciardelli C., Nova I., Tronconi E., Ascherfeld M., Fabinski W. (2007) Combined use of a mass-spectrometer and a UV analyzer in the dynamic study of NH_3-SCR for diesel exhaust aftertreatment, *Topics Catal.* **42-43**, 1-4, 161-164.

15 Nova I., Colombo M., Tronconi E., Weibel M., Schmeisser V. (2011) The NH_3 Inhibition Effect in the Standard SCR Reaction of NO over a Fe-zeolite Catalyst: an Experimental and Modeling Study, *SAE Technical Paper* 2011-01-1319.

16 Mears D.E. (1971) Tests for Transport Limitations in Experimental Catalytic Reactors, *Ind. Eng. Chem. Process. Des. Dev.* **10**, 4, 541-547.

17 Forzatti P., Lietti L., Tronconi E. (2003) Nitrogen Oxides Removal, in *Encyclopedia of Catalysis*, Wiley, New York, pp. 298-343.

18 Buzzi Ferraris G., Donati G. (1974) A powerful method for Hougen-Watson model parameter estimation with integral conversion data, *Chem. Eng. Sci.* **29**, 6, 1504-1509.

19 Beeckman J.W. (1991) Measurement of the effective diffusion coefficient of nitrogen monoxide through porous monolith-type ceramic catalysts, *Ind. Eng. Chem. Res.* **30**, 2, 428-430.

20 Koebel M., Elsener M., Madia G. (2001) Reaction pathways in the selective catalytic reduction process with NO and NO_2 at low temperatures, *Ind. Eng. Chem. Res.* **40**, 1, 52-59.

21 Madia, G., Koebel M., Elsener M., Wokaun A. (2002) The effect of an oxidation precatalyst on the NOx reduction by ammonia SCR, *Ind. Eng. Chem. Res.* **41**, 15, 3512-3517.

22 Iwasaki M., Yamazaki K., Shinjoh H. (2009) Transient reaction analysis and steady-state kinetic study of selective catalytic reduction of NO and NO + NO_2 by NH_3 over Fe/ZSM-5, *Appl. Catal. A: Gen.* **366**, 1, 84-92.

23 Kapteijn F., Singoredjo L., Dekker N.J.J., Moulijn J.A. (1993) Kinetics of the selective catalytic reduction of nitrogen oxide (NO) with ammonia over manganese oxide (Mn_2O_3)-tungsten oxide (WO_3)/.gamma.-alumina, *Ind. Eng. Chem. Res.* **32**, 3, 445-452.

24 Koebel M., Elsener M. (1998) Selective catalytic reduction of NO over commercial DeNOx-catalysts: experimental determination of kinetic and thermodynamic parameters, *Chem. Eng. Sci.* **53**, 4, 657-669.

25 Willey R.J., Lai H., Peri J.B. (1991) Investigation of iron oxide-chromia-alumina aerogels for the selective catalytic reduction of nitric oxide by ammonia, *J. Catal.* **130**, 2, 319-331.

26 Nova I., Lietti L., Tronconi E., Forzatti P. (2000) Dynamics of SCR reaction over a TiO_2-supported vanadia-tungsta commercial catalyst, *Catal. Today* **60**, 1-2, 73-82.

28 Malmberg S., Votsmeier M., Gieshoff J., Soger N., Mussmann L., Schuler A., Drochner A. (2007) Dynamic phenomena of SCR-catalysts containing Fe-exchanged zeolites - experiments and computer simulations, *Topics Catal.* **42-43**, 1-4, 33-36.

29 Sjovall H., Blint R.J., Gopinath A., Olsson L. (2010) A Kinetic Model for the Selective Catalytic Reduction of NO_x with NH_3 over an Fe-zeolite Catalyst, *Ind. Eng. Chem. Res.* **49**, 1, 39-52.

30 Brandenberger S., Kroecher O., Tissler A., Althoff R. (2008) The State of the Art in Selective Catalytic Reduction of NOx by Ammonia Using Metal-Exchanged Zeolite Catalysts, *Catal. Rev. Sci. Eng.* **50**, 4, 492-531.

31 Katada N., Igi H., Kim J.H., Niwa M. (1997) Determination of the acidic properties of zeolite by theoretical analysis of temperature-programmed desorption of ammonia based on adsorption equilibrium, *J. Phys. Chem. B* **101**, 31, 5969-5977.

32 Parrillo D.J., Gorte R.J. (1993) Characterization of Acidity in H-Zsm-5, H-Zsm-12, H-Mordenite, and H-Y Using Microcalorimetry, *J. Phys. Chem.* **97**, 34, 8786-8792.

33 Sobalik Z., Jisa K., Jirglova H., Bemauer B. (2007) Simultaneous FTIR/UV-Vis study of reactions over metallo-zeolites Approach to quantitative in situ studies, *Catal. Today* **126**, 1-2, 73-80.

Final manuscript received in May 2011
Published online in September 2011